Cancer Immunol Immunother (2010) 59:989–999
DOI 10.1007/s00262-010-0821-5

ORIGINAL ARTICLE

The anti-tumor effect of Newcastle disease virus HN protein is influenced by differential subcellular targeting

Hong Sui · Yuxian Bai · Kaibing Wang · Xi Li · Chun Song · Fang Fu · Yongxin Zhang · Lejing Li

Received: 29 October 2009 / Accepted: 19 January 2010 / Published online: 4 February 2010

Abstract
Background Immunotherapy is emerging as a major player in the current standard of care for aggressive cancers such as non-small cell lung cancer (NSCLC). The Newcastle disease virus with its tumor-specific replicative and oncolytic abilities is a promising immunotherapeutic candidate. A DNA vaccine expressing the major immunogenic hemagglutinin-neuraminidase (HN) protein of this virus has shown promising results as an immunotherapeutic agent.
Methods In the present study, three different DNA vaccine constructs encoding differentially targeted HN proteins (cytoplasmic or Cy-HN, secreted or Sc-HN and membrane-anchored or M-HN) were generated to evaluate their anti-tumor effect in vitro and in vivo.
Results Although all three DNA constructs elicited an immune response, tumor-bearing mice intratumorally injected with M-HN demonstrated a significantly better anti-tumor effect than those injected with Cy-HN or Sc-HN. We also showed that this anti-tumor effect was mediated by higher lymphocyte proliferative response and CTL activity in mice intratumorally injected with M-HN.
Conclusion The membrane-anchored form of the HN protein appears to be an ideal candidate to develop as an immunotherapeutic agent for NSCLC.

Keywords Non-small cell lung cancer (NSCLC) · Hemagglutinin-neuraminidase (HN) protein · Cellular localization · Anti-tumor effect · CTL activity

H. Sui, Y. Bai and X. Li contributed equally to this work.

H. Sui · Y. Bai · L. Li (✉)
Medical Department, The Tumor Hospital Affiliated Harbin Medical University, Harbin 150040, Heilongjiang, China
e-mail: lilejing1260@126.com

K. Wang
Interventional Department, The Second Hospital Affiliated Harbin Medical University, Harbin, Heilongjiang, China

X. Li · F. Fu · Y. Zhang
Division of Swine Disease,
National Key Laboratory of Veterinary Biotechnology,
Harbin Veterinary Medicine, Harbin, Heilongjiang, China

C. Song
The Key Laboratory of Cell Transplantation of Ministry of Health,
The First Hospital Affiliated Harbin Medical University, Harbin, Heilongjiang, China

Introduction

Non-small cell lung cancer (NSCLC) accounts for approximately 80% of all cases of lung cancer [1], with >60% of patients presenting with locally advanced or metastatic (stage III/IV) disease at initial diagnosis. Conventional treatments such as surgery, radiotherapy and chemotherapy have limited value in curbing the progression of aggressive forms of lung cancer. However, with increasing understanding of the immune processes in cancer, new approaches in cancer treatment use immunotherapeutic strategies such as targeted antibody delivery, the use of cytokines and "cancer vaccines". Monoclonal antibodies targeting cell surface receptors (i.e., cetuximab, bevacizumab) have been approved by the US Food and Drug Administration and are currently being used in the treatment of lung cancer.

In recent years, there has been an active interest in the potential use of replication-competent oncolytic viruses as therapeutic agents in the treatment of cancer [2–6]. One such virus is the Newcastle disease virus (NDV) which

belongs to the Paramyxoviridae family of RNA viruses and infects all species of birds [7, 8]. Recent reports demonstrated that the highly purified, replication-competent D90 strain directly lysed diverse human cancer cells in vitro (oncolytic) while being significantly less toxic toward normal human cells [9]. Intralesional NDV caused complete tumor regression in athymic mice with a high therapeutic index [10].

The oncolytic mechanism of NDV is known to be mediated via its hemagglutinin-neuraminidase (HN) and fusion proteins (F) which are targeted to the surface of tumor cells infected with the virus. The induction of T cell costimulatory activity and cytokine production enhances tumor-specific antigen expression which results a specific anti-tumor response. Previous studies showed that the HN but not the F protein induced IFN-alpha and TRAIL in peripheral blood mononuclear cells [11]. Antibodies against HN but not F were able to block these responses. The exact mechanism by which these viruses selectively target tumor cells is not well-understood.

However, the oncolytic efficiency of many naturally occurring NDV strains can be relatively low and many tumors exhibit strong innate immune responses that suppress viral replication and spread. In fact, some murine tumor model systems were shown to generate anti-NDV antibodies which counteracted oncolysis mediated presumably by lymphocytes [12]. Some groups focused on developing a recombinant strain of the virus to modulate innate immune responses in order to optimize its oncolytic properties [13–15].

The aim of our study was to use a rational molecular design to enhance the anti-tumor effect of the HN protein of NDV. We designed three different expression plasmids encoding the HN protein targeted to different subcellular compartments: cytoplasmic (Cy-HN), secreted (Sc-HN) and membrane-anchored (M-HN). We developed a mouse model in order to evaluate the anti-tumor effect of the intratumorally injected modified HN proteins. Our data clearly showed that the membrane-anchored form of HN generated a more efficient anti-tumor effect than the secreted or cytoplasmic forms.

Materials and methods

Cells and viruses

The human lung carcinoma cell line A549 was obtained from the Harbin Veterinary Medicine Research Institute of the Chinese Academy of Agricultural Sciences and maintained in Dulbecco's modified Eagle's medium (DMEM, Invitrogen, USA), supplemented with 10% (v/v) heat-inactivated fetal bovine serum (Invitrogen, USA), 100 μg/ml streptomycin and 100 IU/ml penicillin (both obtained from the Harbin General Pharmaceutical Factory, China). The NDV strain D90 used in this study was obtained from the Harbin Veterinary Medicine Research Institute of the Chinese Academy of Agricultural Sciences and propagated in allantoic fluid.

Construction and purification of plasmids

DNA vaccine constructs expressing three different versions of the HN protein were cloned in a pcDNA3.1(+) expression vector (Invitrogen, USA). Full length and truncated versions of the HN gene were amplified using genomic DNA of the D90 strain of NDV as a template in a high-fidelity PCR reaction. PCR cycling conditions were as follows: denaturation at 94°C for 5 min followed by 35 cycles of 94°C for 50 s, 56.3°C for 50 s, 72°C for 150 s. Final elongation was at 72°C for 8 min. The Cy-HN expression vector (the cytoplasmic targeted protein) was created by PCR amplification of a 1,716-bp DNA fragment representing the full-length protein using the primer pair HNs/HNr (Table 1). The PCR product was digested with *Eco*RI/*Eco*RV and subcloned in pcDNA3.1(+) using standard protocols. The Sc-HN expression vector (the secreted protein) was created by PCR amplification of the full-length HN fragment. This was then digested with *Eco*RI And *Eco*RV and subcloned into pcDNA3.1-tPA, a modified pcDNA3.1(+) containing the tissue plasminogen activator (tPA) leader sequence which increases secretion efficiency [16]. The M-HN expression vector (the membrane-anchored protein) was created by PCR amplification of the HN fragment without a stop codon, using primer pair HN′s/HN′r. This 1,713-bp fragment was subcloned into pcDNA3.1-tPA, resulting in pcDNA3.1-tPA-HN′. A 126-bp DNA fragment containing the transmembrane anchor domains (TM) of influenza virus hemagglutinin (HA) was PCR amplified from genomic DNA of the influenza A virus using the primer pair HA1/HA2 designed from the appropriate GenBank sequence (GenBank accession: AF461521). After digestion with *Eco*RV and *Xho*I, this PCR product was cloned into pcDNA3.1-tPA-HN′, immediately downstream of the HN gene. A schematic of these recombinant plasmids is shown in Fig. 1. All plasmids were verified by appropriate restriction enzyme digestion and sequencing.

Transfections, indirect immunofluorescence assay and sodium dodecyl sulfate (SDS)-PAGE

Six-well tissue culture plates (BD, USA) were seeded with A549 cells at a concentration of 4×10^5 cells/well. Cells were grown to approximately 80–90% confluence. All transient transfections were carried out using LipofectAMINE

Table 1 Oligonucleotide primers used in this study

Primer	Sequences (5′ → 3′)	Fragment size (bp)
HNs	CCGGAATTCATGGACCGCGCGGTTAACAGAG	1,716
HNr	CGATATCTTAAACTCTATCATCCTTGAGG	
HN′s	CCGGAATTCATGGACCGCGCGGTTAACAGAG	1,713
HN′r	CGATATCAACTCTATCATCCTTGAGGATCTC	
HA1	CGGATATCCAAACTTACCAAATACT	126
HA2	CTCGAGCGGTTAAATGCAAATTC	

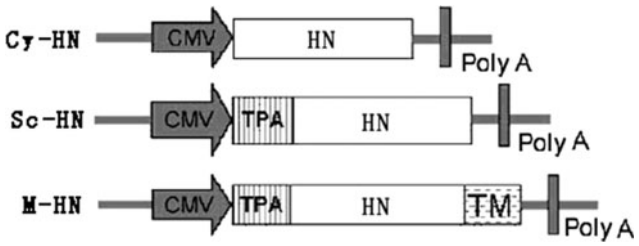

Fig. 1 Plasmids used for expression analysis in vitro and for DNA treatment. pcDNA3.1(+) was used to express three different versions of HN encoding cytoplasmic (Cy-HN), secreted (Sc-HN) and membrane-anchored (M-HN) HN protein, respectively. *CMV* cytomegalovirus immediate-early promoter/enhancer, *TPA* tissue plasminogen activator signal sequence, *polyA* polyadenylation signal, *TM* the transmembrane anchor domains (TM) of influenza virus HA, *HN* HN gene of new castle disease virus strain D90. The *boxed arrows* show the position of the CMV promoter and direction of transcription

2000 reagent (Invitrogen, USA) according to the manufacturer's instructions. At 48-h post-transfection, the cells were fixed with absolute methanol and processed for indirect immunofluorescence assay using homemade mouse anti-NDV polyclonal antibodies (1:100), followed by FITC-conjugated rabbit anti-mouse IgG (1:80) (Sigma, USA). Fluorescent images were examined under an inverted fluorescence microscope (Olympus IX70). For protein analysis, cells were harvested at 48-h post-transfection and washed three times with PBS. The cell pellet was then resuspended in 100 μl deionized water, mixed with an equal volume of 2× SDS sample buffer [0.1 M Tris–Cl (pH 6.8), 20% (m/v) glycerol, 4% (m/v) SDS, 3.1% (m/v) DTT, 0.001% (m/v) bromophenol blue] and boiled for 10 min. Twenty microliters of each lysate was electrophoresed on a 12% SDS-polyacrylamide gel.

MTT cell viability assay

The MTT cell viability assay and growth curves were used to measure the inhibitory effects of recombinant HN protein on the proliferation of A549 cells. Cells were plated at a density of 8×10^3 cells/well in 96-well tissue culture plates and transfected with 0.25 μg of the plasmids Cy-HN, Sc-HN or M-HN. Cells transfected with empty vector pcDNA3.1 and untransfected cells were used as controls. At 48-h post-transfection, cell viability was determined by incubating the cells with 25 μl of MTT solution [5 mg/ml in phosphate buffer (PBS, pH 7.2) and filtered] for 4 h at 37°C. DMSO (200 μl) was added to each well to dissolve the formazan product produced by viable cells. The optical density was read at 570 nm using an automated microplate reader (Bio-Tek Instruments, Inc., VT, USA). To normalize for differences in cell densities, a WST-1 assay was performed in parallel on the same plate. The results determined in five wells were adjusted to cell numbers.

Apoptosis assay

Six-well plates were seeded with single-cell suspensions of A549 cells (5×10^5 cells/ml). Cells were transfected as described above and incubated for 24 or 72 h at 37°C. Cells were harvested by trypsinization and resuspended in PBS. Cells were stained with a TACS annexin V-FITC kit (R&D Systems, USA) and apoptosis was evaluated using a FACScan flow cytometer (BD Biosciences, USA). Results were analyzed using CellQuest version 3.1f software (BD Biosciences, USA). Propidium iodide-negative cells that stained positively with annexin V were considered to be apoptotic. The difference between early and late apoptotic cells was analyzed using flow cytometry by Annexin V-PI assay. Electron microscopy was used to capture representative images of apoptotic bodies. Apoptotic and morphological changes were identified by AO/PI double staining and subsequent visualization using a confocal laser scanning microscope (CLSM).

Establishment of a mouse model bearing human lung carcinoma and intratumoral injection schedule

We used 6–8-week-old female, athymic homozygous nu/nu BALB/c mice purchased from the Shanghai Slac Laboratory Animal Company, Shanghai, China. Mice were housed in groups of four or five per cage and were maintained at 22°C, 55% relative humidity and a 12-h light/dark cycle. All experiments were carried out under the guidelines of the Laboratory Protocol of Animal Handling, Harbin Medical University. Tumors were established by subcutaneous injection of 3×10^6 A549 cells in 150 μl of PBS into the

outer thigh of athymic nude mice. Solid tumors became visible after 5–6 days and tumor sizes were determined as the product of the perpendicular diameters of the tumors at 2–3-day intervals. Tumor volumes were estimated as follows: volume = (square root of maximal tumor cross-sectional area)^3 [17]. Once tumors reached at least 25 mm in any one dimension, mice were randomized into five treatment groups and intratumorally injected with 100 μg of Cy-HN, Sc-HN, M-HN, the empty vector pcDNA3.1(+) plasmids and physiological saline. Treatment was administered every 5 days over a period of 15 days (days 1, 5, 10, 15) as previously described [18]. All animals were killed 21 days after treatment was initiated and none of the mice developed symptoms such as weight loss or dyscrasia.

Lymphocyte proliferative response

Mouse lymphocytes were prepared as follows. Spleens from the immunized mice were homogenized in 1:4 (v/v) of PBS (pH 7.4). The erythrocytes were lysed with 0.75% Tris–NH_4Cl (pH 7.4). After three washes with PBS, single-cell suspensions of lymphocytes were purified from splenocytes with Ficoll-isopaque solution and were resuspended at a density of 1×10^7 cells/ml in RPMI 1640 containing 10% FBS, 14 mM HEPES, 50 mM 2-mercaptoethanol, 100 μg/ml streptomycin and 100 IU/ml penicillin. The lymphocytes were plated in 96-well flat-bottom plates at 100 μl/well (1×10^6 cells/well). Subsequently 100 μl of medium with or without HN antigen (5 μg/ml) was added to each well and mixed. Concanavalin A (5 μg/ml; Sigma, USA) was used as a positive control. Each lymphocytes sample was plated in triplicate. The proliferative response was measured using a modification of the MTT (3-(4,5-dimethylthiazol-2-yl)-2,5-diphenyltetrazolium bromide) assay. Briefly, after 72 h of incubation, 20 μl of MTS (3-(4,5-dimethylthiazol-2-yl)-5-(3-carboxymethoxyphenyl)-2-(4-sulfophenyl)-2H-tetrazolium, inner salt; Promega, USA) was added to each well and plates were incubated for a further 5 h. At the end of the incubation, the plates were read at 570 nm. The stimulation index (SI) was calculated as the ratio of the average OD value of wells containing antigen-stimulated cells to the average OD of wells containing cells treated with only medium.

CTL assay

A standard 4-h ^{51}Cr release assay [19] was used to measure CTL activity in vitro. Briefly, single-cell suspensions of lymphocytes were prepared from spleens in complete RPMI 1640 medium (containing 10% heat-inactivated FBS, 2 mM L-glutamine, 1 mM sodium pyruvate, 1% penicillin–streptomycin–Fungizone, 1% non-essential amino acids, 1% HEPES buffer, and 5×10^{-5} M 2-ME) and used as effector cells. Experimental and control effector lymphocytes were boosted in vitro for 96 h at 37°C with mitomycin C-treated A549 tumor cells. The in vitro-boosted effector cells were washed, and resuspended in complete RPMI medium. ^{51}Cr-labeled A549 cells were dispensed in triplicate in a 96-well U-bottom microtiter plates (BD) at a density of 2×10^4 cells/well. Different ratios of effector cells:tumor cells (75:1, 50:1 and 25:1) were dispensed in a total volume of 200 μl/well. Tumor cells were also incubated alone (spontaneous release) or with 50 μl of Zapoglobin (Beckman Coulter) lytic reagent (total release). The plate was incubated at 37°C for 4 h and centrifuged at 800 rpm for 6 min before harvesting 100 μl of the supernatant from each well and estimating chromium release on a gamma counter. Cytotoxicity was determined by the amount of ^{51}Cr released by the target cells using a (Model Cobra II, Packard Instrument Company). Specific lysis was calculated as follows: [(experimental cpm) − (spontaneous release cpm)]/[(maximum release cpm) − (spontaneous release cpm)] × 100%.

Statistical analyses were performed using SPSS™ software

All data were expressed as mean ± standard deviation (SD). One-way analysis of variation (one-way ANOVA) was used to test if differences in cell death rate, tumor size, SI and specific lysis transfected by the different constructs were statistically significant. The difference among time-points was examined by one-way ANOVA as well. When the measurement at one time-point was dependent on others, one-way ANOVA was supplanted with a linear mixed model. Once a significant result was revealed by one-way ANOVA or linear mixed model, Fisher's LSD was then utilized for post hoc tests. As long as the assumption of equal SD in all groups was violated, Dunnett's T3 test was applied to post hoc tests. A two-sided P value < 0.05 was defined as statistically significant. All statistics were computed with SPSS statistical software (version 15.0, SPSS Inc., Chicago, IL, USA).

Results

Plasmid design and localization analysis

Figure 1 depicts the construction of three different versions of the HN protein targeted to different subcellular compartments. Cy-HN contained the full-length HN gene, resulting in a cytoplasmic localized form of the HN protein. In order to create a secreted form of HN (Sc-HN), the human tPA leader sequence, a strong signal peptide for protein secretion [16] was cloned immediately upstream of the full-length HN gene. The membrane-anchored form of HN (M-HN)

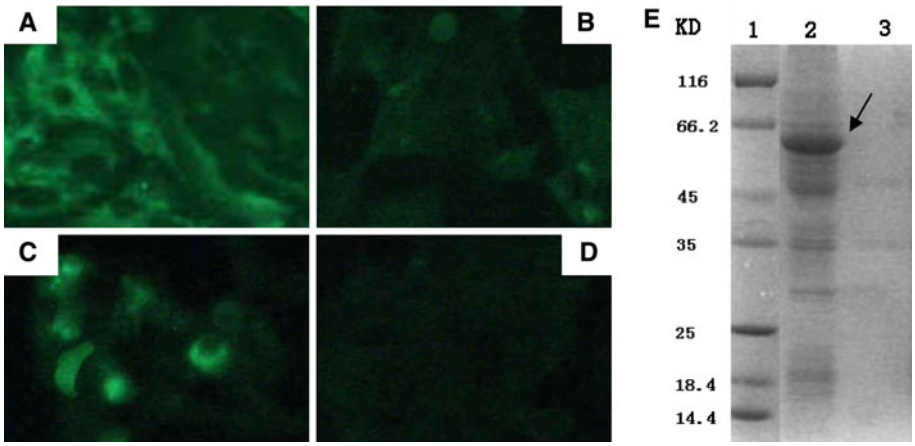

Fig. 2 Expression and intracellular localization analyses of modified HN protein in transfected A549 cells. Approximately 80–90% confluent A549 cells were transfected with 4 μg of plasmid DNA. At 48-h post-transfection, the cells were fixed with absolute ethanol and processed for an indirect immunofluorescence assay. Representative fluorescence images of cells transfected with Cy-HN (**a**), Sc-HN (**b**), M-HN (**c**) or the empty vector pcDNA3.1(+) (**d**) are shown. For SDS-PAGE (**e**), cell lysates (*lane 3*) or supernatants (*lane 2*) from cells transfected with Sc-HN were prepared at 48-h post-transfection. *Arrow* indicates the expressed HN protein

contained the transmembrane domain of the HA gene in addition to the tPA leader sequence. In order to verify the differential targeting of the three versions of the HN protein, 80–90% confluent A549 cells were transfected with Cy-HN, Sc-HN, M-HN, or the empty vector pcDNA3.1(+), respectively, and an indirect immunofluorescence assay was performed. There was no fluorescence observed in pcDNA3.1(+)-transfected cells (Fig. 2d). Cy-HN-transfected cells showed a cytoplasmic localization of HN in the majority of the transfected cells (Fig. 2a). M-HN-transfected cells showed a clear and strong fluorescence at the cell surface (Fig. 2c). Although there was little immunofluorescence in Sc-HN-transfected cells (Fig. 2b), SDS-PAGE analysis demonstrated that the expressed protein of the expected size was found mainly in the supernatant of Sc-HN-transfected cells (Fig. 2e), indicating that transfection of cells with the Sc-HN construct resulted in efficient secretion of HN to the supernatant. These results demonstrated that the modified HN gene was expressed efficiently and targeted into the expected cell compartments of the transfected cells.

Recombinant HN protein induces cell death in A549 cells in vitro

Figure 3 shows the percentage of cell death induced by the three differentially targeted HN proteins in A549 cells. We found that the percentage of cell death was maximal in M-HN-transfected cells at 24-h post-transfection while maximal cell death was observed in Sc-HN-transfected cells at 48-h post-transfection. We did not find any statistically significant differences in cell death induced by the three versions of HN at 72-h post-transfection ($P = 0.056$).

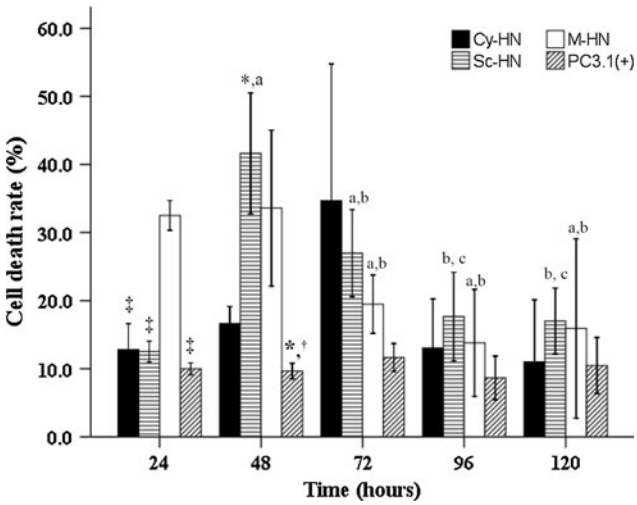

Fig. 3 Cell death rate in A549 cells transfected with Cy-HN, Sc-HN, M-HN or the empty vector pcDNA3.1(+) for 120 h ($n = 3$ or 4 per group). One-way ANOVA followed by LSD or Dunnett's T3 test was performed to test for differences among the four subcellular localizations at a specific time-point and the difference between five time-points for a given subcellular localization (significantly different from Cy-HN, $^{*}P < 0.05$; significantly different from Sc-HN, $^{\dagger}P < 0.05$; significantly different from M-HN, $^{\ddagger}P < 0.05$; *a* indicates significantly different from 24 h; *b* indicates significantly different from 48 h; *c* indicates significantly different from 72 h). Data are presented as mean ± standard deviation (SD)

When kinetics of cell death were charted, we found that Sc-HN caused maximal cell death at 48 h and this declined significantly at 96 h. Kinetics of cell death in M-HN-transfected cells showed a peak between 24 and 48 h and then significantly decreased at 72 h and maintained plateaued thereafter.

Recombinant HN protein induces apoptosis of A549 cells in vitro

A549 cells transfected with the plasmids encoding the three differentially targeted HN proteins were evaluated for apoptosis using FCM. Figure 4 demonstrates that the percentage of apoptosis induced in A549 cells at 24-h post-transfection (right lower quadrant) by Cy-HN, Sc-HN, M-HN or the empty vector pcDNA3.1(+) was 30.13, 39.29, 49.59 and 4.70%, respectively. The percentage of total apoptosis (the sum of the right lower quadrant and right upper quadrant) at 72-h post-transfection for the same set of transfected cells was 48.27, 94.2, 54.56 and 4.80%, respectively (Fig. 4).

Detection of apoptotic bodies using electron microscopy and AO/PI double-staining CLSM

Using electron microscopy and AO/PI double staining, we demonstrated (Fig. 5b) that apoptosis was mainly seen during the early stages (lower right quadrant) while necrosis was seen at later stages (upper right quadrant). We also used electron microscopy to show the presence of apoptotic bodies in A549 cells transfected with Sc-HN, Cy-HN and M-HN (Fig. 5a).

The effect of differentially targeted HN protein on A549 tumor growth in vivo

Mice carrying lung tumors derived from A549 cells were treated with intratumoral injections of the three different versions of the HN DNA vaccine constructs. Table 2 shows the variation in tumor size among animals treated with the differently targeted HN constructs. At Day 9, the tumor size of negative control animals treated with PC3.1(+) was significantly larger than M-HN. On Days 12, 15 and 18, the saline-treated as well as PC3.1(+)-treated animals also exhibited larger tumor sizes than HN-treated animals. At Day 21, we found that the largest tumor size was in the saline-treated animals followed by PC3.1(+)-treated animals followed by Cy-HN, Sc-HN and M-HN, respectively.

As expected, when the mice were evaluated between Days 18 and 21 after the primary intratumoral injection, we observed the highest anti-tumor effect in M-HN injected mice compared with other groups (at 18-day timeline: $P = 0.022$ for M-HN; at 21-day timeline: $P < 0.01$ for M-HN).

Differentially targeted HN DNA constructs influence the proliferative activity of splenocytes differently

The effect of the three differentially targeted forms of HN on the proliferative response of splenocytes was measured using the MTT assay. As shown in Fig. 6, the highest SI was detected in M-HN-injected mice and the lowest SI was observed in PC3.1(+)-injected mice (2.18 vs. 0.87, $p = 0.003$).

M-HN elicits a more robust CTL activity in tumor-bearing mice when compared to Sc-HN or Cy-HN

The ability of $CD8^+$ T cells (CTLs) to lyse tumor cells in the setting of our differentially targeted HN DNA vaccines was measured using a standard CTL assay. As expected, BALB/c mice injected subcutaneously with HN-transfected A549 tumor cells developed CTLs that effectively lysed these A549 tumor cells but failed to lyse the empty vector-transfected A549 tumor cells, indicating that A549 tumor cells were susceptible to lysis by allogeneic CTLs. We referred to these $CD8^+$ T cells as "$CD8^+$ anti-tumor effector cells" rather than "CTLs". We showed (Fig. 7) that mice injected intratumorally with M-HN demonstrated significantly higher CTL activity (mainly $CD8^+$ T cells) compared with mice injected intratumorally with Cy-HN, Sc-HN or PC3.1(+) vector at 75:1 E/T ratio. This difference was statistically significant when compared with Cy-HN, Sc-HN or PC3.1(+) vector ($P = 0.019$, $P = 0.043$, $P < 0.01$, respectively) at 75:1 E/T ratio. There was no significant difference between the Cy-HN group and Sc-HN groups ($P = 0.656$). Specific lysis induced by the differently targeted constructs at a 75:1 E/T ratio was ranked as PC3.1(+) < Sc-HN < M-HN. Furthermore, in the M-HN group, higher specific lysis was seen at a 75:1 E/T ratio when compared to a ratio of 25:1.

Discussion

Strategies using immunological approaches to elicit an anti-tumor response have emerged as an attractive approach to treat cancers such as NSCLC where mortality statistics have not improved much in more than 20 years. Although lung cancer was not originally considered an immune-sensitive malignancy, there is increasing evidence that specific humoral and cellular anti-tumor immune responses can be evoked during the course of this disease. With the emergence of data proposing a beneficial role for chemotherapy and radiation in the production of anti-tumor immune response, it increasingly appears that immunotherapy could become an important component of the current standard of care for NSCLC.

Creating an efficacious vaccine involves selection of the most appropriate tumor antigens and formulation of their immunogenic epitopes into a construct for delivery to antigen-presenting cells. Clinical trials employing immunotherapy to treat NSCLC showed that there was a strong induction of an immune response augmenting the clinical

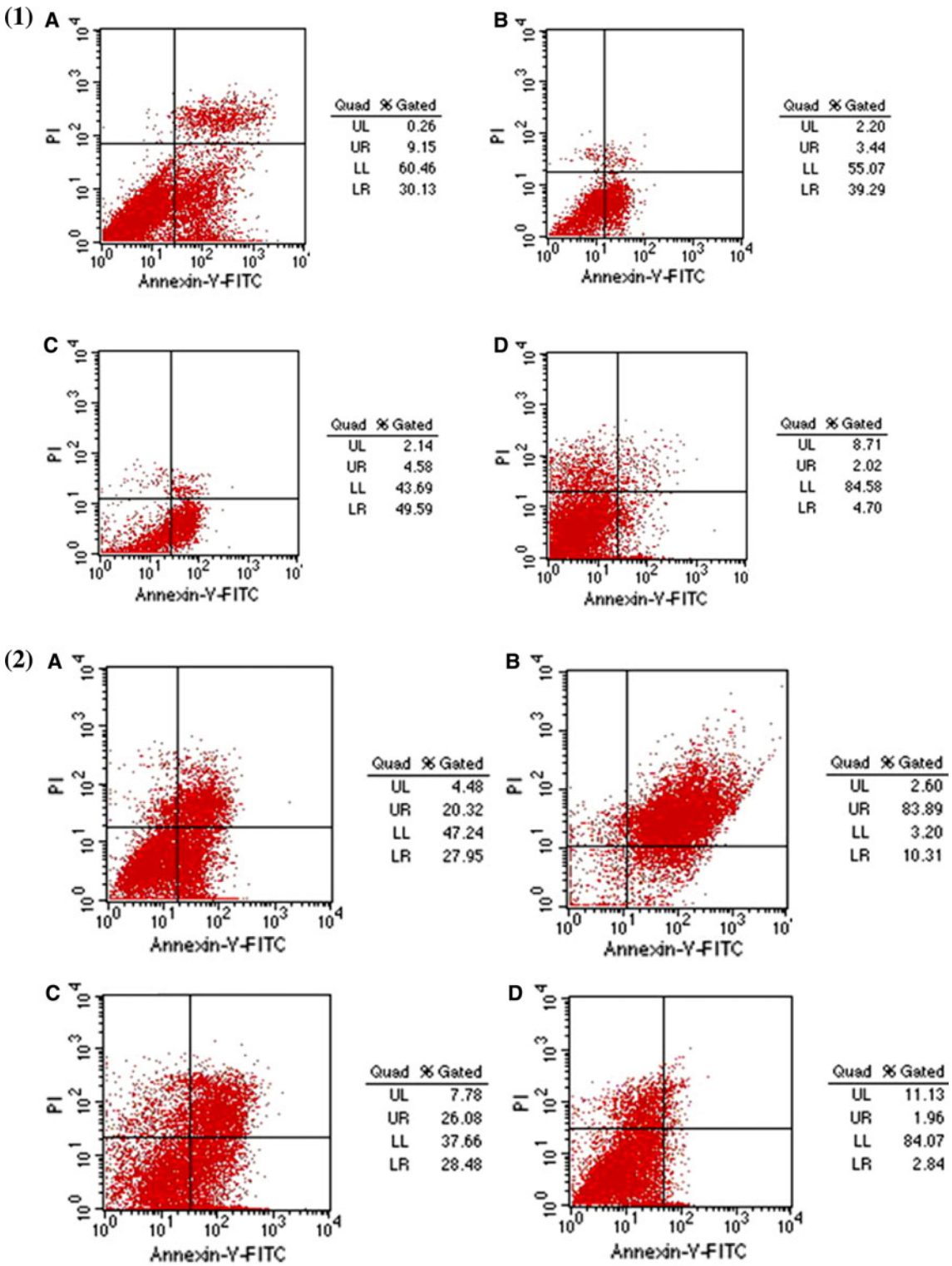

Fig. 4 Detection of apoptosis of A549 by flow cytometry. Approximately 80–90% confluent A549 cells were transfected with 4 μg of plasmid DNA in six-well tissue culture plates. At 24-h (**1**) or 72-h (**2**) post-transfection, the cells were collected and stained with a TACS annexin V-FITC kit as described

responses seen when compared with controls treated with standard therapy [20]. NDV, an enveloped, cytoplasmic RNA virus with a very restricted host range belongs to the family Paramyxoviridae and was found to have an intrinsic oncolytic activity associated with it [21]. NDV was found to effectively and selectively replicate in and kill tumor

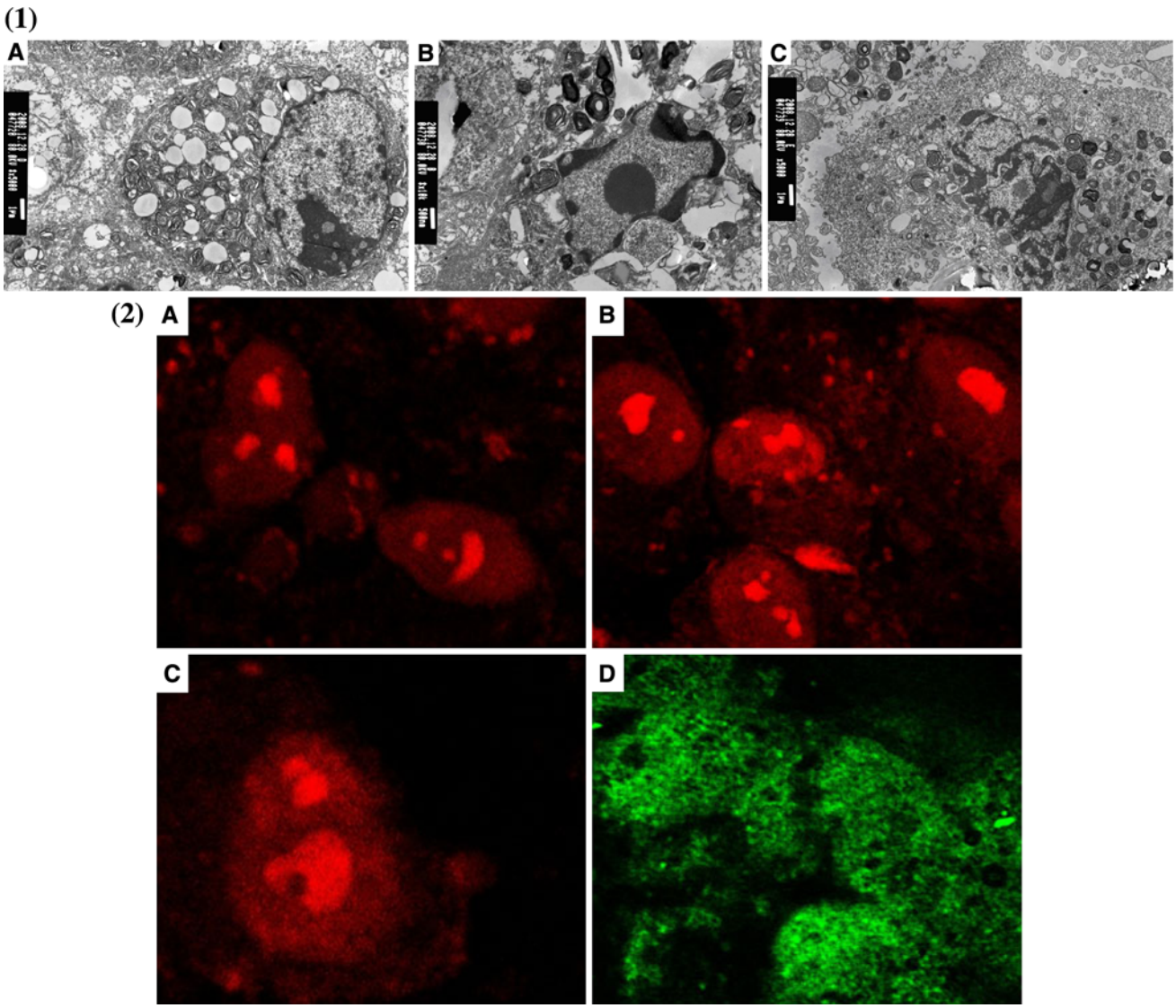

Fig. 5 Representative images of apoptotic bodies. **1** Demonstration of apoptotic bodies in A549 cells induced by Cy-HN (*a*), Sc-HN (*b*) and M-HN (*c*) by electron microscopy. **2** AO/PI double staining of A549 cell after transfection with Cy-HN (*a*), Sc-HN (*b*), M-HN (*c*) and the empty vector pcDNA3.1(+) (*d*) by CLSM

cells but not normal cells. The NDV infectious particle uses its functional HN protein to bind specific host cell receptors while the fusion protein (F) mediates the fusion of the viral envelope to the host cell membrane. Introduction of the HN protein (1,000 molecules per virus particle) into the tumor cell facilitates cell–cell interactions and elicits a strong CTL response. It was shown that NDV caused an upregulation of the tumor-specific cytotoxic CD8 T cell (CTL) response as well as an increased CD4 T-helper cell activity in the absence of an antiviral response [22].

However, the exact mechanism by which the HN gene induces oncolysis has not been elucidated. The neuraminidase activity of HN is known to hydrolyze sialic acid residues on the host cell surface causing the receptor to be exposed and subsequent viral replication-independent induction of TRAIL (tumor necrosis factor-related apoptosis inducing ligand) expression in peripheral blood monocytes/lymphocytes. The HN protein also induced the formation of a special recognition site on the membrane of tumor cell that enhanced tumor cell recognition by the immune system followed by a cytotoxic response [11, 23].

We elected to investigate the immunogenicity of the HN protein in the context of its subcellular compartmentalization within the host cell. Our objective was to manipulate the localization of this protein in order to change its immunogenicity to modulate tumor cell recognition and cytotoxicity by the host immune system. Our data suggest that targeting the

Table 2 Variation of tumor size of A549 lung carcinoma tumor in 40 mice between 6 and 21 days

Day[a]	Mean ± SD					P[b]	Post hoc test[c]
	Group 1: PC3.1(+) (n = 8)	Group 2: Cy-HN (n = 8)	Group 3: Sc-HN (n = 8)	Group 4: M-HN (n = 8)	Group 5: physiological saline (n = 8)		
6	22.8 ± 2.4[a]	20.9 ± 3.6[a]	21.4 ± 2.1[a]	20.7 ± 1.6[a]	23.0 ± 3.5[a]	0.336	NA
9	27.0 ± 3.5[b]	23.9 ± 1.6[b]	23.8 ± 1.7[b]	22.4 ± 0.8[b]	25.2 ± 3.4[b]	0.007*	G1 > G4
12	32.4 ± 0.2[c]	26.1 ± 1.0[c]	26.6 ± 2.0[c]	25.1 ± 0.9[c]	31.8 ± 0.3[c]	<0.001*	G2 = G3 = G4 < G5 < G1
15	32.3 ± 1.8[c]	27.3 ± 0.5[c]	27.0 ± 1.2[c]	25.9 ± 2.1[c]	33.4 ± 1.7[c]	<0.001*	G2 = G3 = G4 < G1 = G5
18	36.9 ± 0.7[d]	31.8 ± 0.8[d]	32.0 ± 3.9[d]	29.4 ± 1.4[d]	36.5 ± 1.2[d]	<0.001*	G4 < G2 < G3 < G1 = G5
21	42.0 ± 1.6[e]	34.0 ± 0.8[e]	34.8 ± 1.3[e]	32.7 ± 0.3[e]	44.2 ± 0.1[e]	<0.001*	G4 < G2 = G3 < G1 < G5

Different letters meant significant differences between various time-points, $P < 0.05$

SD standard deviation, *Cy-HN* cytoplasmic HN, *Sc* secreted HN, *M* membrane-anchored HN, *NA* not available

[a] Linear mixed model was implemented to examine the differences between the time-points studied

[b] One-way ANOVA was performed

[c] LSD test or Dunnett's T3 test was used

* Significantly different among all groups, $P < 0.05$

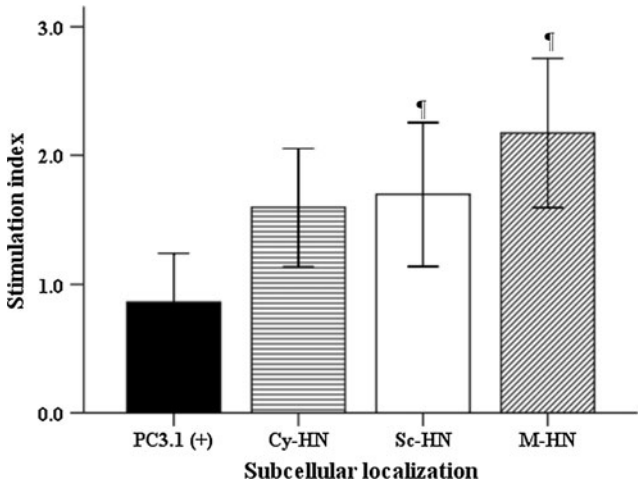

Fig. 6 Stimulation index in A549 cells transfected with PC3.1(+), Cy-HN, Sc-HN and M-HN (n = 4 per group). One-way ANOVA was used; LSD was utilized for post hoc tests. Significantly different from PC3.1(+), $^{¶}P < 0.05$. Data are presented as mean ± standard deviation (SD)

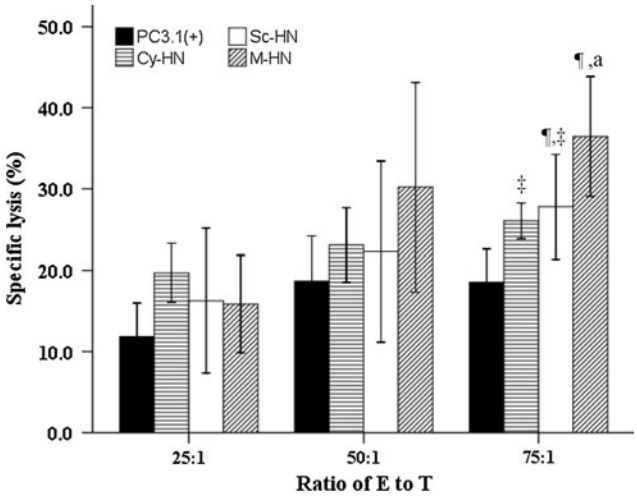

Fig. 7 The CTL activity in tumor-bearing mice treated with PC3.1(+), Cy-HN, Sc-HN and M-HN (n = 4 per group). One-way ANOVA followed by LSD or Dunnett's T3 test was performed to test the difference between the four subcellular localizations at a specific E/T ratio and the difference between the three E/T ratios for each subcellular localization. Significantly different from PC3.1(+), $^{¶}P < 0.05$. Significantly different from M-HN, $^{‡}P < 0.05$. *a* indicates significantly different from E/T ratio of 25:1, $P < 0.05$. Data are presented as mean ± standard deviation (SD)

HN protein to different subcellular compartments influences both the humoral and cellular immune responses.

We found that growth inhibition of A549 cells was maximal with the secreted form of HN in the group treated for less than 48 h. This effect was statistically significant when compared to the membrane-anchored or the cytoplasmic forms of HN. However, growth inhibition of A549 cells was higher in the M-HN group at 24 h while there was no statistically significant difference among the three groups between 72 and 120 h. We speculate that the modified HN protein in the transfected A549 cells could enhance cell mortality of A549 cells or effect a change in the kinetics of the growth curve. The presence of apoptotic bodies correlated with the MTT cell viability assay when we evaluated the inhibitory effects of the different forms of HN on A549 cells.

Based on the data from the MTT and FCM assays, we concluded that the anti-tumor effect of the HN protein could be manipulated by differential subcellular targeting. Although it is possible that plasmid processing and protein localization may differ in vitro from an in vivo situation, it is noteworthy that the membrane-anchored form of HN intratumorally injected into tumor-bearing mice inhibited tumor growth more effectively than did the cytoplasmic

or secreted versions of the HN protein. We propose to follow-up on these data with immunohistochemistry and immunoblotting experiments in our animal model in order to determine subcellular localization in vivo. All the DNA constructs elicited an efficient immunogenic response leading us to propose that the HN protein in all its versions is processed and presented efficiently on the cell surface in agreement with previous results [23].

We evaluated the proliferative activity of splenocytes after restimulation in vitro with recombinant HN protein. Our results showed enhanced cellular immunity in mice that were intratumorally injected with M-HN when compared to mice injected with Sc-HN or Cy-HN. M-HN induced a significantly higher CTL activity. We demonstrated that these were mainly $CD8^+$ T cells and that this difference was statistically significant ($P < 0.01$). The difference between the Cy-HN and Sc-HN groups was not statistically significant ($P > 0.05$).

Most models of tumor rejection describe $CD8^+$ T cells as the primary mediators of tumor rejection [24–26] acting through the direct recognition of MHC class I to achieve cytolysis. In some models of tumor rejection, $CD4^+$ T cells function as helper cells that are needed only for the induction of CTLs [27–29]. Once $CD8^+$ T cells are primed, the effector function of the CTLs is unaffected by the depletion of $CD4^+$ T cells [30]. We speculate that the modified HN protein induces efficient antigen processing and presentation of the expressed antigens, resulting in high levels of IFN-γ response especially in the case of M-HN [23].

In summary, we demonstrated that the immunogenicity of the HN protein can be significantly enhanced by a molecular design that alters the subcellular localization of the expressed antigen. We draw this conclusion from the fact that the membrane-bound form of the HN protein exerted a stronger anti-tumor effect when compared with the secreted or cytoplasmic forms, although we do not have direct evidence in this report of plasmid processing and subcellular localization in vivo. It is possible that our data could be interpreted differently in light of the fact that the mechanisms of plasmid processing, subcellular localization and mechanisms of immunogenicity in vitro may not be faithfully reflected in vivo. However, our results suggest that the M-HN construct is the best anti-tumor vaccine candidate to study and develop further as an immunotherapeutic anti-tumor agent. While our present study only demonstrates the potential of M-HN in a small animal model, its anti-tumor effect on human tumor xenografts warrants further investigation. We would also like to investigate the effect of cytokines such as IFN and TNF in anti-tumor immune responses. We expect the addition of immunotherapy as a non-toxic adjunct to increase treatment success rates over those obtained with traditional regimens alone.

References

1. Parkin DM, Bray F, Ferlay J, Pisani P (2005) Global cancer statistics, 2002. CA Cancer J Clin 55:74–108
2. Heise C, Hermiston T, Johnson L et al (2000) An adenovirus E1A mutant that demonstrates potent and selective systemic antitumoral efficacy. Nat Med 6:1134–1139
3. Khuri FR, Nemunaitis J, Ganly I et al (2000) A controlled trial of intratumoral ONYX-015, a selectively-replicating adenovirus, in combination with cisplatin and 5-fluorouracil in patients with recurrent head and neck cancer. Nat Med 6:879–885
4. Nakano K, Todo T, Chijiiwa K, Tanaka M (2001) Therapeutic efficacy of G207, a conditionally replicating herpes simplex virus type 1 mutant, for gallbladder carcinoma in immunocompetent hamsters. Mol Ther 3:431–437
5. Stojdl DF, Lichty B, Knowles S et al (2000) Exploiting tumor-specific defects in the interferon pathway with a previously unknown oncolytic virus. Nat Med 6:821–825
6. Yu DC, Chen Y, Seng M, Dilley J, Henderson DR (1999) The addition of adenovirus type 5 region E3 enables calydon virus 787 to eliminate distant prostate tumor xenografts. Cancer Res 59:4200–4203
7. Herold-Mende C, Karcher J, Dyckhoff G, Schirrmacher V (2005) Antitumor immunization of head and neck squamous cell carcinoma patients with a virus-modified autologous tumor cell vaccine. Adv Otorhinolaryngol 62:173–183
8. Phuangsab A, Lorence RM, Reichard KW, Peeples ME, Walter RJ (2001) Newcastle disease virus therapy of human tumor xenografts: antitumor effects of local or systemic administration. Cancer Lett 172:27–36
9. Fu F, Liu C-y, Rui G, Yang B-f, Song C, Li X (2008) Anti-tumor effects of NDV D90 against tumor cells of A549 in vitro. Chin J Prevent Vet Med 30:179–182, 189
10. Donahue JM, Mullen JT, Tanabe KK (2002) Viral oncolysis. Surg Oncol Clin N Am 11:661–680
11. Zeng J, Fournier P, Schirrmacher V (2002) Induction of interferon-alpha and tumor necrosis factor-related apoptosis-inducing ligand in human blood mononuclear cells by hemagglutinin-neuraminidase but not F protein of Newcastle disease virus. Virology 297:19–30
12. Sinkovics JG, Howe CD (1969) Superinfection of tumors with viruses. Experientia 25:733–734
13. Bian H, Fournier P, Moormann R, Peeters B, Schirrmacher V (2005) Selective gene transfer in vitro to tumor cells via recombinant Newcastle disease virus. Cancer Gene Ther 12:295–303
14. Janke M, Peeters B, de Leeuw O et al (2007) Recombinant Newcastle disease virus (NDV) with inserted gene coding for GM-CSF as a new vector for cancer immunogene therapy. Gene Ther 14:1639–1649
15. Zamarin D, Martinez-Sobrido L, Kelly K et al (2009) Enhancement of oncolytic properties of recombinant newcastle disease virus through antagonism of cellular innate immune responses. Mol Ther 17:697–706
16. Tong T, Fan H, Tan Y et al (2006) C3d enhanced DNA vaccination induced humoral immune response to glycoprotein C of pseudorabies virus. Biochem Biophys Res Commun 347:845–851
17. Grzelinski M, Steinberg F, Martens T, Czubayko F, Lamszus K, Aigner A (2009) Enhanced antitumorigenic effects in glioblastoma on double targeting of pleiotrophin and its receptor ALK. Neoplasia 11:145–156

18. Wei L, Dai J, Sun S (2000) Construction of Newcastle disease virus hemagglutinin-neuraminidase (HN) gene and its antitumor immune response effects. Acad J Second Military Med Univ 21:6
19. Hegde S, Niederkorn JY (2000) The role of cytotoxic T lymphocytes in corneal allograft rejection. Invest Ophthalmol Visual Sci 41:3341–3347
20. Holt GE, Disis ML (2008) Immune modulation as a therapeutic strategy for non-small-cell lung cancer. Clin Lung Cancer 9(Suppl 1):S13–S19
21. Cassel WA, Garrett RE (1965) Newcastle disease virus as an antineoplastic agent. Cancer 18:863–868
22. Schirrmacher V, Haas C, Bonifer R, Ertel C (1997) Virus potentiation of tumor vaccine T-cell stimulatory capacity requires cell surface binding but not infection. Clin Cancer Res 3:1135–1148
23. Fan H, Xiao S, Tong T et al (2008) Immunogenicity of porcine circovirus type 2 capsid protein targeting to different subcellular compartments. Mol Immunol 45:653–660
24. Cho JS, Hsu JV, Morrison SL (2009) Localized expression of GITR-L in the tumor microenvironment promotes CD8+ T cell dependent anti-tumor immunity. Cancer Immunol Immunother 58:1057–1069
25. Klyushnenkova EN, Kouiavskaia DV, Berard CA, Alexander RB (2009) Cutting edge: permissive MHC class II allele changes the pattern of antitumor immune response resulting in failure of tumor rejection. J Immunol 182:1242–1246
26. Zitvogel L, Mayordomo JI, Tjandrawan T et al (1996) Therapy of murine tumors with tumor peptide-pulsed dendritic cells: dependence on T cells, B7 costimulation, and T helper cell 1-associated cytokines. J Exp Med 183:87–97
27. Qin Z, Richter G, Schuler T, Ibe S, Cao X, Blankenstein T (1998) B cells inhibit induction of T cell-dependent tumor immunity. Nat Med 4:627–630
28. Ridge JP, Di Rosa F, Matzinger P (1998) A conditioned dendritic cell can be a temporal bridge between a CD4+ T-helper and a T-killer cell. Nature 393:474–478
29. Schoenberger SP, Toes RE, van der Voort EI, Offringa R, Melief CJ (1998) T-cell help for cytotoxic T lymphocytes is mediated by CD40–CD40L interactions. Nature 393:480–483
30. Umeshappa CS, Huang H, Xie Y et al (2009) CD4+ Th-APC with acquired peptide/MHC class I and II complexes stimulate type 1 helper CD4+ and central memory CD8+ T cell responses. J Immunol 182:193–206